Time Dependent Neutronics Analysis for the First Wall of the University of Wisconsin Heavy Ion Beam Fusion Reactor Design

M.E. Sawan, G.A. Moses, G.L. Kulcinski

October 1980

UWFDM-386

Trans. ANS 38 (1981) 574, Nucl. Tech./Fusion 2 (1982) 215.

FUSION TECHNOLOGY INSTITUTE

UNIVERSITY OF WISCONSIN

MADISON WISCONSIN

Time Dependent Neutronics Analysis for the First Wall of the University of Wisconsin Heavy Ion Beam Fusion Reactor Design

M.E. Sawan, G.A. Moses, G.L. Kulcinski

Fusion Technology Institute
University of Wisconsin
1500 Engineering Drive
Madison, WI 53706

http://fti.neep.wisc.edu

October 1980

UWFDM-386

Trans. ANS 38 (1981) 574, Nucl. Tech./Fusion 2 (1982) 215.

Time Dependent Neutronics Analysis for the First Wall of the University of Wisconsin Heavy Ion Beam Fusion Reactor Design

Mohamed E. Sawan

Gregory A. Moses

Gerald L. Kulcinski

Fusion Engineering Program
Nuclear Engineering Department
University of Wisconsin
Madison, WI 53706

October 1980

UWFDM-386

Abstract

Time dependent neutronics analysis for the ferritic steel first wall of the University of Wisconsin heavy ion beam fusion reactor conceptual design is presented. Neutron target interactions which lead to spectrum softening and neutron multiplication are accounted for. The time of flight spread of neutrons within each energy group is considered. Neutron slowing down in the porous tube first wall protection system is found to significantly affect the time over which the damage occurs in the first wall. In the case of an unprotected wall, the time spread is determined primarily by the time of flight spread. Using the porous tube first wall protection concept is found to significantly reduce both average and peak instantaneous rates of dpa, helium production, and energy deposition in the first wall.

I. Introduction

Neutronics studies form a vital part of a fusion reactor system design. Important parameters such as tritium breeding ratio, neutron energy deposition, and radiation damage to the first wall and structure can be calculated by performing detailed neutronics calculations. In a magnetic confinement fusion reactor, the fusion reactions that produce neutrons will be sustained for a time which is much longer than the time of flight spread and the neutron slowing down time in the blanket. Furthermore, no neutron fuel interactions occur in the relatively low density ($\sim 10^{14}/cm^3$) plasma. Therefore, steady state neutronics calculations with a thermally broadened 14.1 MeV neutron source will be sufficient for a magnetic confinement fusion reactor.

In an inertial confinement fusion reactor the neutron source has a pulsed nature because of the very short burn time over which the fusion reactions occur (10-100 ps). Furthermore, the neutron pulse does not reach the first surface of the blanket until ~ 100 ns after the burn and the neutron slowing down time in the blanket is much greater than the duration of the neutron source. Significant softening of the energy spectrum of neutrons escaping from the target results from neutron interaction with the dense ($\sim 10^{26}/cm^3$) fuel and surrounding tamper material. This leads to a considerable time of flight spread as neutrons reach the first surface. Therefore, time dependent neutronics studies are essential for the proper analysis of inertial confinement fusion reactors.

As a result of the pulsed nature of the neutron source, high instantaneous damage rates are present in an inertial confinement fusion reactor wall and structure. This can lead to significant changes in the microstructure[1] of the first wall material. It has also been found that high

instantaneous dpa (displacements per atom) rates result in higher recombination rates with the void growth being inhibited and swelling decreased.[2] Accurate instantaneous damage rates can be calculated by performing time dependent neutronics studies. Previous time dependent neutronics studies have been used to calculate the instantaneous dpa rate in the first wall of a laser fusion reactor[3] and an electron beam fusion reactor.[4] No correction for the time of flight spread of neutrons within each energy group was made in these studies.

In this work a modified version of the time dependent discrete ordinates code TDA[5] is used to perform time dependent neutronics analysis of the University of Wisconsin heavy ion beam (HIB) fusion reactor conceptual design. In this design the first wall is protected by an array of porous tubes which contain liquid metal. The tubes are composed of braided silicon carbide through which a lithium-lead liquid metal eutectic flows. Besides protecting the first wall the $Li_{17}Pb_{83}$ eutectic serves as the coolant and the tritium breeder. The effects of the liquid metal protection on the peak instantaneous and average dpa and gas protection rates in the ferritic steel first wall are investigated. The steady state discrete ordinates ANISN[6] code is used to determine the average time integrated radiation damage rates.

Energy deposition in the porous tubes and first wall of the HIB fusion reactor is important in the determination of their structural integrity. The temporal and spatial dependence of energy deposition is also required for stress analysis studies. The energy deposition rate integrated over the volume of the blanket of a laser fusion reactor has been calculated in a previous study.[7] However, no detailed time dependent fluxes or energy deposition rates at different points were given. In this work, we calculate the

instantaneous energy deposition rates at different positions in the blanket and first wall.

II. Heavy Ion Beam Reactor Computational Model

The reactor utilizes a spherical pellet similar to that reported by Bangerter and Meeker[8] with the TaCOH pusher replaced by a mixture of lithium and lead having the same density. At ignition the compressed pellet is assumed to have a DT fuel ρR of 2 g/cm^2 and a pusher ρR of 1 g/cm^2.

The pellet ignites at the center of a cylindrical reactor cavity which has a radius of 7 m and a height of 10 m. The blanket region has a thickness of 2 m (30% of which is devoted to the porous tubes) and it is placed in front of the first wall. The blanket consists of an array of tubes made of braided SiC through which a $Li_{17}Pb_{83}$ eutectic flows. The $Li_{17}Pb_{83}$ coolant represents 80 vol % and the SiC structural material represents 20 vol % of the porous tubes. The blanket region has an effective thickness of 60 cm. SiC and $Li_{17}Pb_{83}$ have nominal densities of 3.17 and 9.4 g/cm^3, respectively.

The first wall is 1 cm thick and is made of a ferritic steel (HT-9) which is an alloy composed of 85.25 wt % iron and 11.5 wt % chromium in addition to other constituent elements. A density of 7.8 g/cm^3 is used for ferritic steel. A reflector with a thickness of 40 cm is used and it consists of 90 vol % ferritic steel structural material and 10 vol % $Li_{17}Pb_{83}$ coolant. The reactor utilizes a 3.5 m thick concrete shield. The shield is not included in the neutronics calculations presented here and appropriate albedos are used to account for possible backscattering from the shield.

A schematic of the blanket, first wall, reflector, and shield configuration for the heavy ion beam fusion reactor is given in Fig. 1. The nuclide densities used in the calculations are given in Table 1. The results

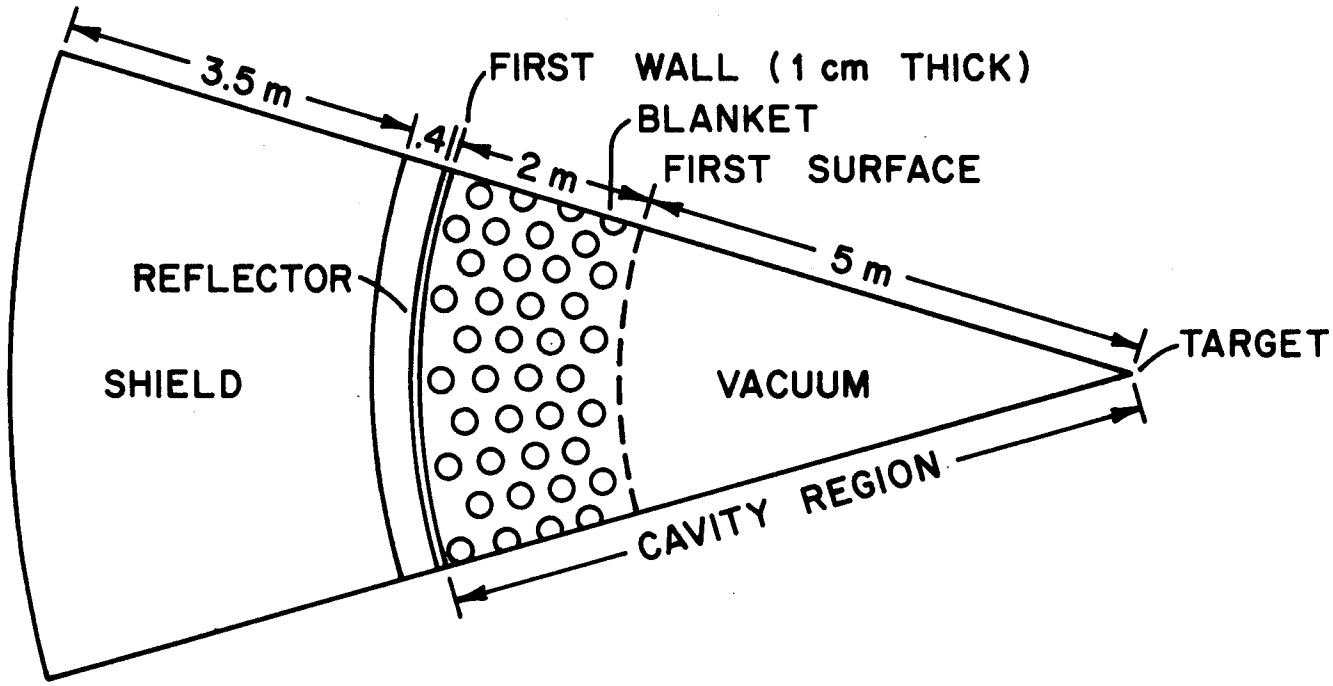

Fig. 1 HIB reactor cavity model.

Table 1

Nuclide Densities Used in Neutronics Analysis of HIB Fusion Reactor

Region	Constituent Elements	Nuclide Density (nuclei/b cm)
Blanket	^{6}Li	.00033
[80 v/o $Li_{17}Pb_{83}$	^{7}Li	.00412
+ 20 v/o SiC]	Si	.00953
(.3 density factor)	C	.00953
	Pb	.02172
Ferritic Steel	Fe	.07174
First Wall	Cr	.01725
(1.0 density factor)	Ni	.00066
	Mo	.00081
	V	.00046
	Si	.00069
	Mn	.00071
	C	.00130
	W	.00022
Reflector	Fe	.06456
[90 v/o ferritic steel	Cr	.01553
+ 10 v/o $Li_{17}Pb_{83}$]	Ni	.00060
(1.0 density factor)	Mo	.00073
	V	.00041
	Si	.00063
	Mn	.00064
	C	.00117
	W	.00020
	^{6}Li	.00004
	^{7}Li	.00051
	Pb	.00272

presented here for the damage and energy deposition rates are based on a DT yield of 400 MJ which corresponds to 1.42×10^{20} source neutrons per pulse. A repetition rate of 5 Hz is used to determine the total dpa and helium production in the first wall per full power year (FPY).

The steady state discrete ordinates code ANISN is used to perform detailed neutronics and photonics calculations within the pellet, giving the time integrated energy spectrum of neutrons escaping from the pellet. This spectrum is used as a source for the time dependent neutronics analysis in the blanket performed using the time dependent multi-group discrete ordinates code TDA. ANISN is used to calculate the time integrated reaction rates. Since the particle transport codes used are one-dimensional, spherical geometry is used in the blanket calculations and hence the results represent the worst conditions at the central plane of the cylindrical reactor. A P3-S8 approximation is used in the transport calculations. A coupled 25 neutron-21 gamma group cross section library is used throughout this work. This library consists of the RSIC DLC-41B/VITAMIN-C data library[9] and the DLC-60/MACKLIB-IV response data library.[10]

III. Neutron Source

The pellet, though absolutely very small, is an extremely dense medium composed primarily of light elements. This results in a substantial collision probability for fusion neutrons created in the pellet. The 14.1 MeV fusion neutrons are degraded in energy as a result of elastic collisions with the fuel (DT) and inelastic collisions with the high Z materials (Pb). Neutron multiplication results also from (n,2n) and (n,3n) reactions with the constituent elements of the pellet. Since the neutrons escaping from the pellet represent the neutron source for the blanket neutronics calculations, it is

essential to perform detailed neutronics calculations for the pellet to accurately account for spectrum softening and neutron multiplication.

Since the burn time of the pellet (10-100 ps) is much greater than the slowing down time of fusion neutrons in the extremely dense pellet (~ .1 ps), steady state calculations yield useful information. Furthermore, since the burn time is much smaller than the time neutrons take to reach the first surface of the blanket and the time of flight spread, neutrons are assumed to be emitted in a pulse with zero time duration ($\delta(t)$). This implies that the time integrated spectrum of the neutrons leaking from the pellet as calculated by the steady state code ANISN gives the correct neutron source spectrum. In other words, if $n_L(E,t)$ is the exact spectrum of neutrons leaking from the pellet at time t within the burn, the time integrated spectrum calculated by ANISN is given by

$$n_L(E) = \int_{t_B} n_L(E,t)dt \ , \qquad (1)$$

where t_B is the burn time. Since the burn time is very small, all neutrons leaking at different times during the burn are assumed to be emitted at t=0 and the source for the blanket calculations is given by

$$S(E,t) = n_L(E)\ \delta(t) \ . \qquad (2)$$

Since the pellet has a very small radius compared to the radius of the reactor cavity, the neutron source is represented by a point source at the center of the reactor. Furthermore, neutrons are emitted isotropically from the pellet and the complete representation of the neutron source is given by

$$S(\mu,r,E,t) = n_L(E)\ \delta(r)\ \delta(t)\ \delta(\mu-1)\ . \qquad (3)$$

Detailed neutronics and photonics calculations have been performed for the HIB fusion reactor pellet. A complete description of the results together with the pellet hydrodynamics and radioactivity results will be presented later. The results show that a pellet neutron multiplication of 1.046 is obtained. This results mainly from (n,2n) reactions in the dense DT fuel core and LiPb pusher. The average energy of neutrons leaking from the pellet is found to be 11.98 MeV implying that 71.2% of the fusion energy is carried by the emerging neutrons.

The spectrum of neutrons leaking from the pellet, $n_L(E)$, is given in Fig. 2. A large peak at 14.1 MeV is attributed to fusion neutrons escaping without interacting with the pellet materials. This amounts to ~ 71% of neutrons leaking. The peaks at 2 and 4 MeV are caused by backward elastic scattering with D and T in the fuel region.

As neutrons travel from the pellet to the first surface of the blanket considerable time of flight spreading occurs because of the broad energy distribution of these neutrons. The arrival time spectrum at the first surface located 5 m from the neutron source is shown in Fig. 3. The numbers at the bottom of the graph indicate the energy groups associated with the various times. Since all neutrons in a specified energy group are forced by the multigroup treatment of the neutronics code to travel at the same velocity corresponding to the average group energy, these neutrons will arrive at the first surface simultaneously and no time of flight spread corresponding to the energy group width will be observed. In order to preserve the correct arrival time spectrum at the first surface given in Fig. 3, we give source neutrons

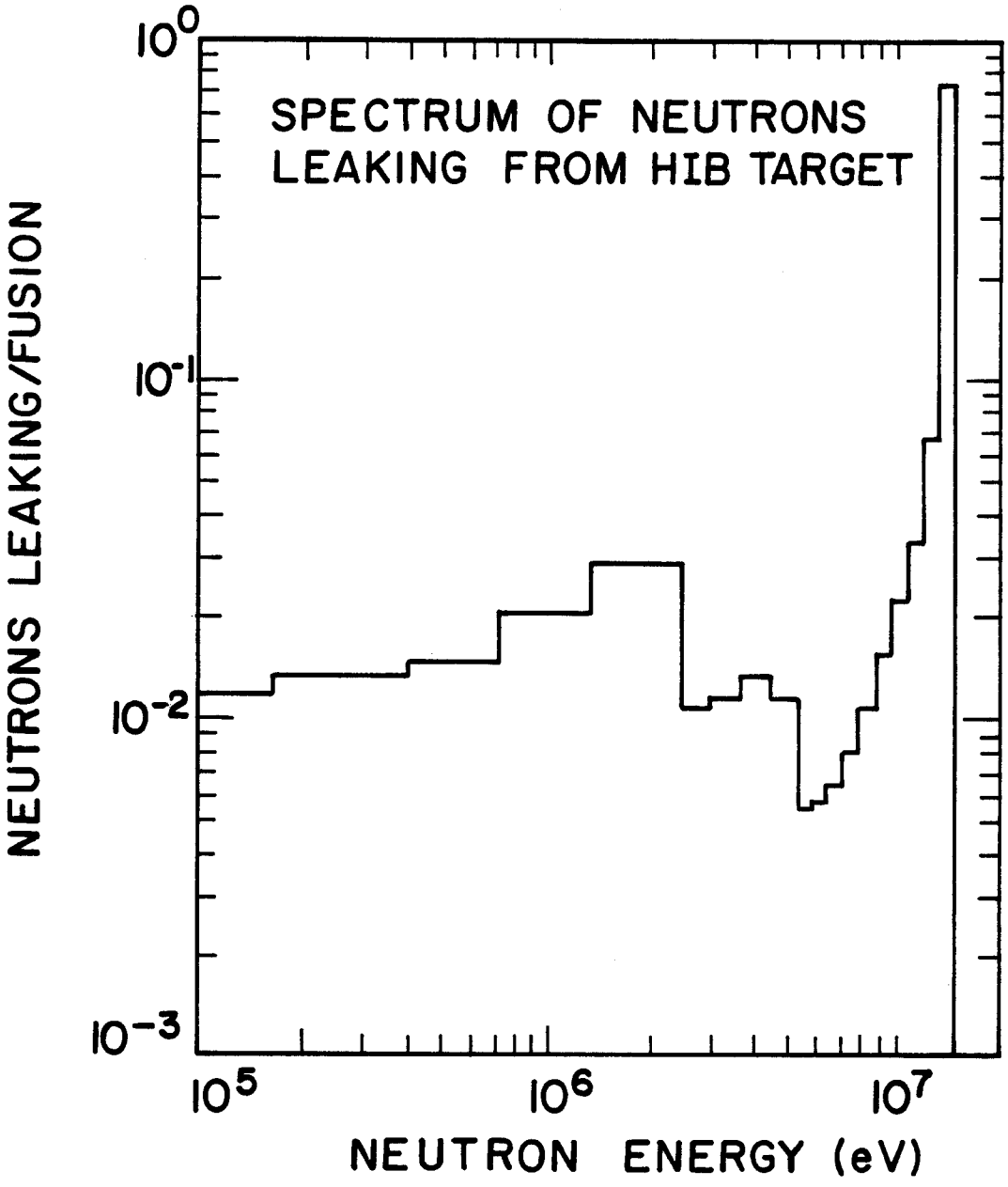

Fig. 2 Spectrum of neutrons leaking from HIB target.

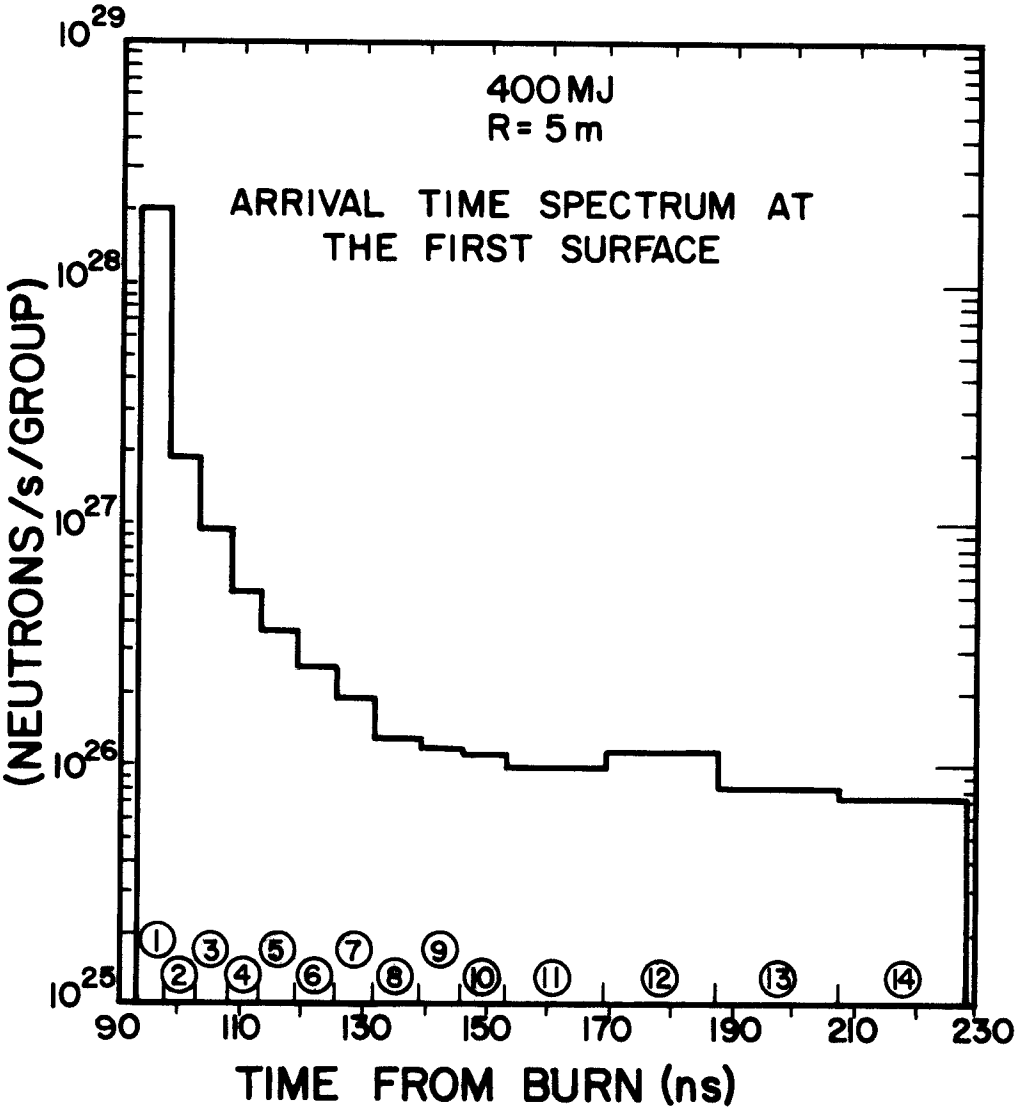

Fig. 3 Arrival time spectrum at the first surface of the blanket.

artificial birth times associated with their energies within the group. If the time of flight spread corresponding to the gth energy group width is Δ_g, the modified neutron source for group g is represented by a rectangular pulse with a time duration of Δ_g. This necessary correction for time of flight spread of neutrons within each energy group was not made in the previous time dependent neutronics analysis of inertial confinement fusion reactors.[3,4]

IV. Time Dependent Neutron Spectrum in the First Wall

A version of the time dependent multigroup discrete ordinates code TDA, modified to facilitate its use for the analysis of inertial confinement fusion reactors, is used to perform time dependent neutronics and photonics calculations for the HIB blanket and reflector model illustrated in Fig. 1. For comparison, calculations are also made for the case of an unprotected wall.

The source for the problem involves Dirac delta functions which are quite difficult to represent with standard finite difference methods. To circumvent this difficulty the uncollided flux is determined analytically and an analytic first collision source is used by the code to determine the collided part of the flux.

The neutron spectrum in the protected ferritic steel first wall is illustrated in Fig. 4. The results are shown at 10 ns and 70 ns after the uncollided neutrons of the highest energy strike the wall. The neutron spectra in the unprotected wall at different times following the arrival of the leading edge of the pulse at the wall are given in Fig. 5. Comparing the results in Figs. 4 and 5, we notice that significant neutron attenuation occurs in the porous liquid metal tubes.

Neutrons slowed down in the inner blanket region take a relatively long time to reach the first wall. This time depends on the slowing down time of

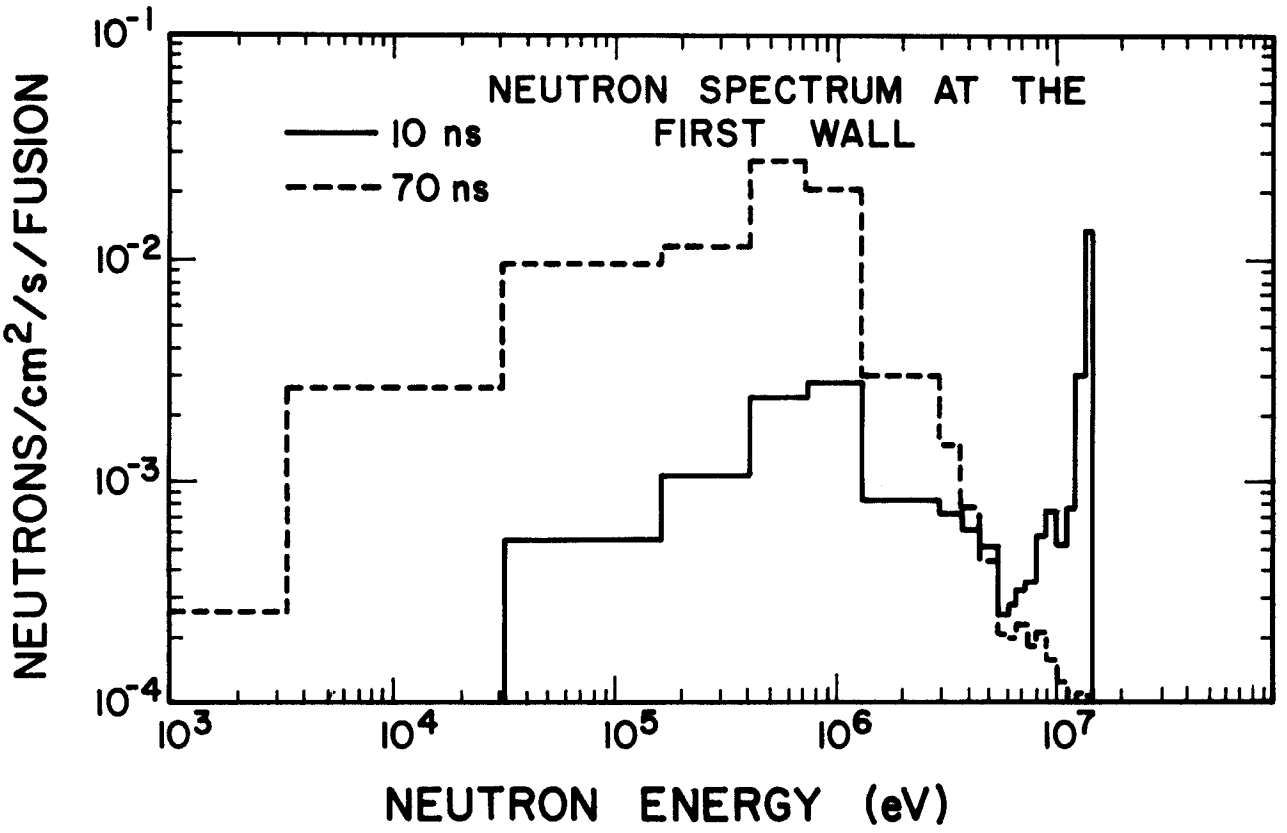

Fig. 4 Neutron spectrum at the HIB first wall.

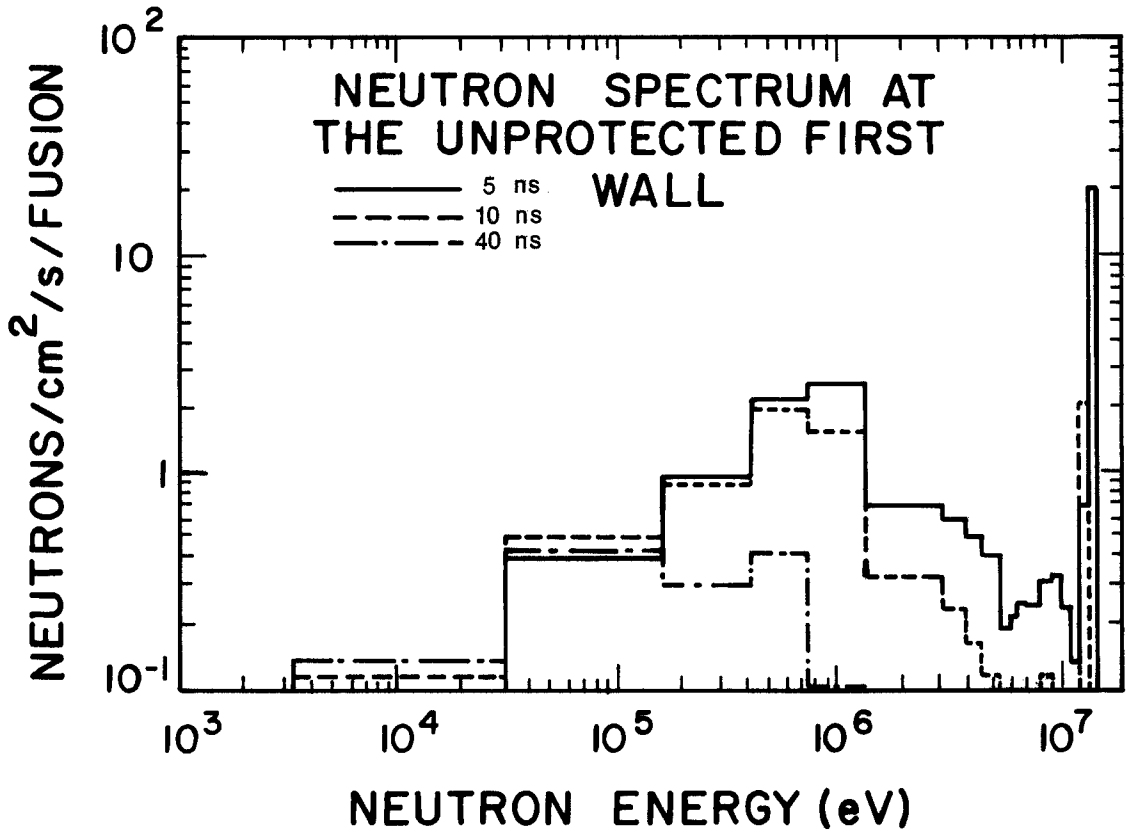

Fig. 5 Neutron spectrum at the unprotected first wall.

neutrons in the blanket, the speed of slowed down neutrons, and the position within the blanket at which the slowing down interaction occurs. At early times, following the arrival of the uncollided fastest neutrons at the first wall, most of the neutrons in the first wall are in the high energy groups. Only neutrons which have been slowed down in the porous tubes close to the first wall are able to arrive at the wall by this time. This effect is enhanced by the neutrons slowed down in the wall itself resulting in the relatively low peak at ~ 1 MeV in Fig. 4. At 60 ns later, most of the high energy neutrons have already passed the first wall while neutrons slowed down in the blanket are still arriving at the first wall primarily because of the relatively long slowing down time of neutrons in the blanket. Therefore, the time dependent spectrum and consequently the instantaneous damage rates in the first wall are governed by two factors; the time of flight spread and the slowing down time spread in the blanket. In lead, which is the main constituent of the blanket, the slowing down time from 14.1 MeV to the inelastic threshold energy of .57 MeV is about 1 μs. At energies below .57 MeV, slowing down is due to elastic scattering with a very small energy loss per collision and this results in much longer slowing down times. Therefore, the time spread of the spectrum in the first wall of our system is determined primarily by the slowing down time in the blanket.

On the other hand, the time of flight spread is the dominant factor in the case of the unprotected wall because of the absence of the "inner" slowing down region. The spectrum at 5 ns after the arrival of the leading edge of the neutron pulse consists mainly of first group neutrons coming directly from the source. The soft part of the spectrum shown in Fig. 5 is due to backward scattering of 14.1 MeV neutrons in the reflector region and neutron slowing

down in the wall itself. As time elapses lower energy source neutrons arrive at the first wall. The effect of neutron slowing down in the reflector is not as pronounced here as compared to the effect of neutron slowing down in the blanket for the case of protected wall. The reason is that the probability of backscattering of high energy neutrons is very small compared to the probability of forward scattering. Therefore, the time dependent damage rate in the unprotected wall is expected to be affected primarily by the time of flight spread.

V. Atomic Displacement Rate

The instantaneous damage rates in the first wall are calculated using the time dependent neutron spectrum in the wall and the appropriate reaction cross sections. The instantaneous dpa rate in the protected ferritic steel first wall is given in Fig. 6. The results correspond to a 400 MJ fusion yield. The cumulative dpa is illustrated in Fig. 7. It is clear that the damage occurs over a relatively long time resulting in a relatively low peak instantaneous dpa rate of 0.014 dpa/s. This considerable time spread results from the relatively long slowing down time in the blanket allowing neutrons of energies greater than the dpa threshold energy of iron ($\sim$ 1 keV) to exist in the first wall over a long period of time.

The instantaneous dpa rate in an unprotected wall is shown in Fig. 8. The time spread is very small compared to the case of the protected wall. The time spread is determined here by the time of flight spread of neutrons as they travel from the source to the wall. The effect of the porous tube protection, used in the University of Wisconsin HIB fusion reactor design, on the atomic displacement in the first wall is given in Table 2. The total dpa per

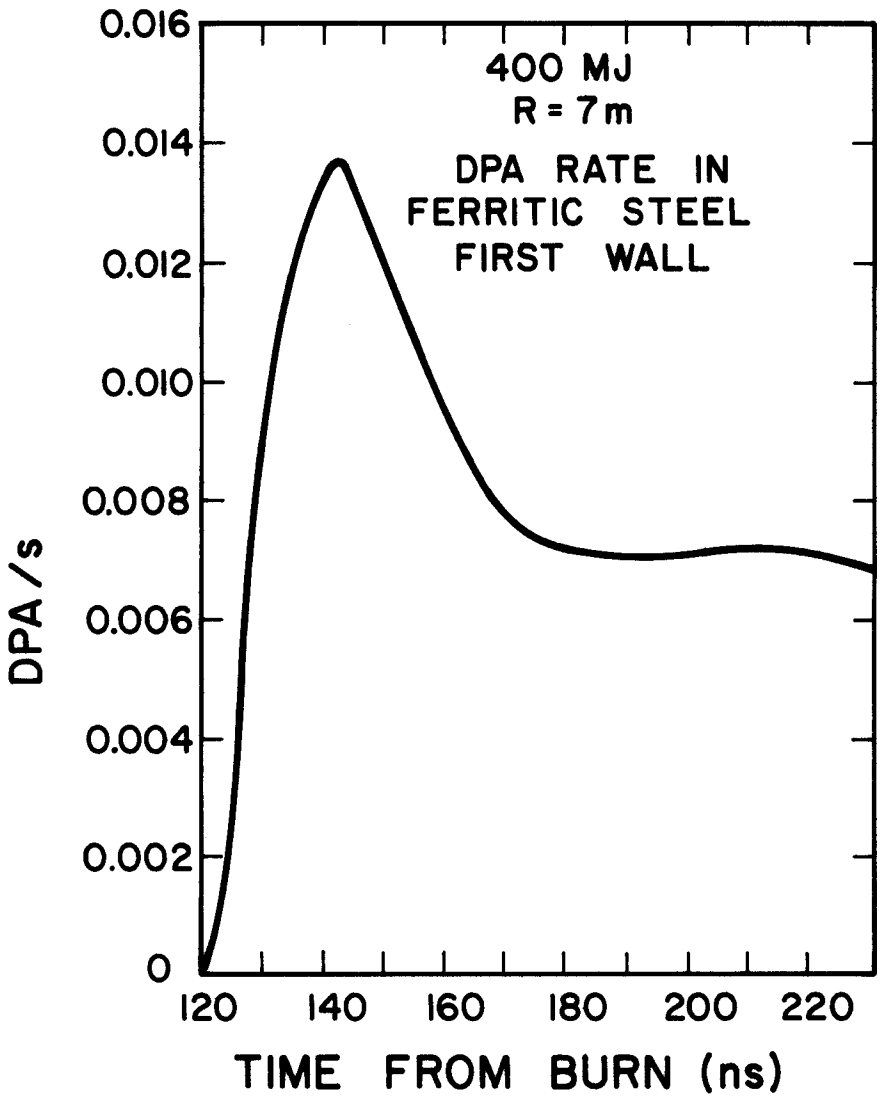

Fig. 6 DPA rate in the protected first wall.

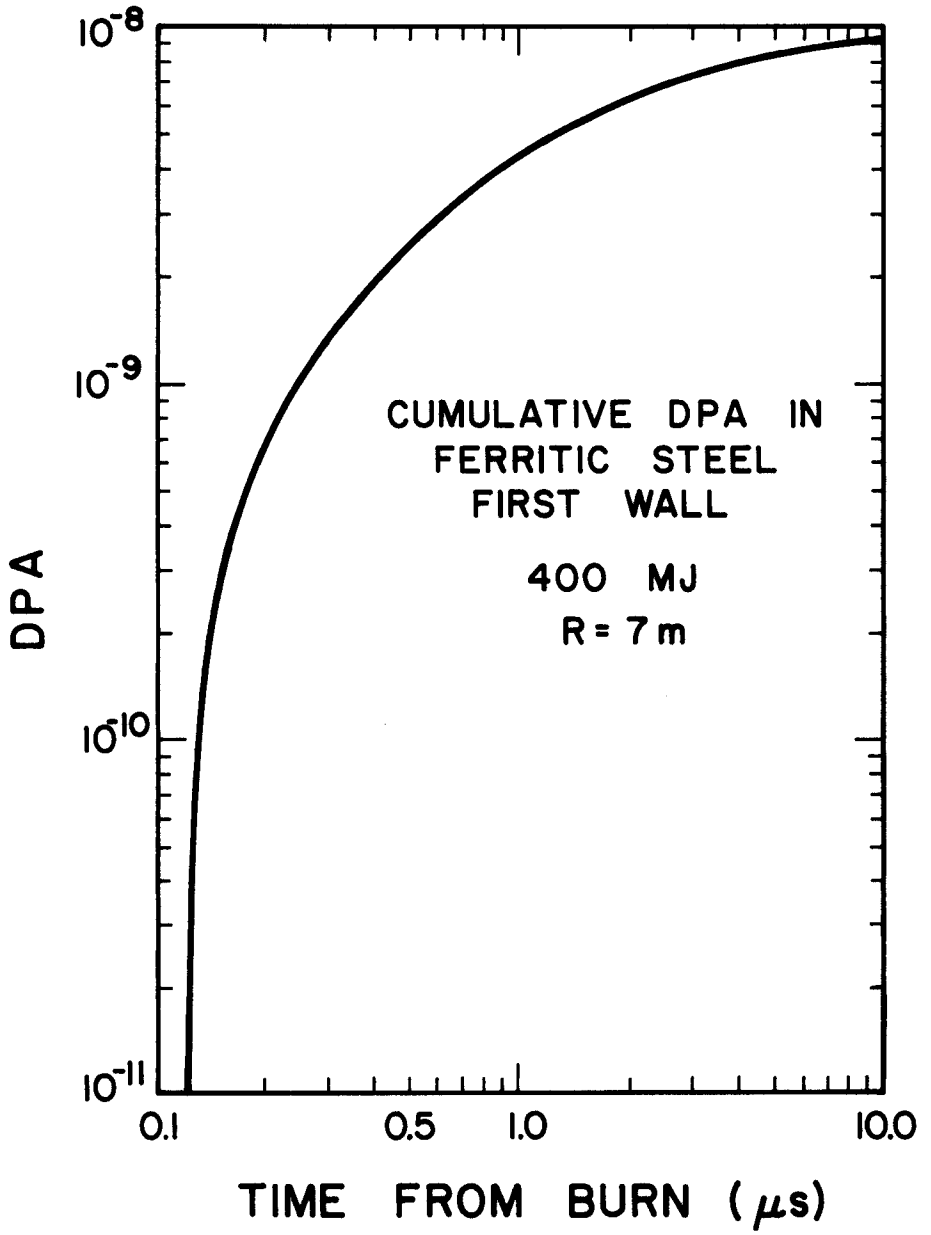

Fig. 7 Cumulative DPA in the protected first wall.

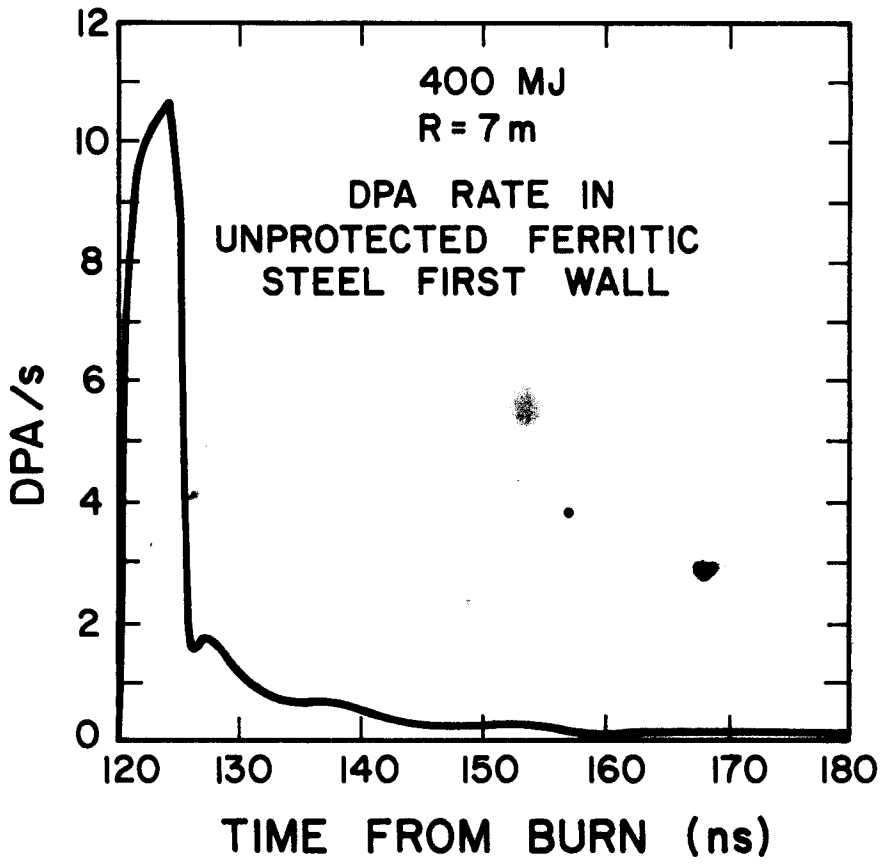

Fig. 8 DPA rate in the unprotected first wall.

full power year (FPY) is determined using the steady state code ANISN with a repetition rate of 5 Hz.

The wall protection used is found to decrease the total cumulative dpa and the peak instantaneous dpa rate by factors of 17 and 780, respectively. The larger reduction in the peak instantaneous dpa rate results from time spread fwhm increasing from 5 to 148 ns. The reduction in dpa achieved here is much larger than that achieved in a SS316 first wall protected by .5 m of liquid Li,[14] typical of the HYLIFE concept. In this case the average rate

Table 2

Effect of First Wall Protection on Atomic Displacement

	Peak Instantaneous dpa rate (dpa/s)	Time Spread fwhm (ns)	Total dpa (dpa/FPY)
Protected Wall	0.0137	148	1.5
Unprotected Wall	10.7	5	25.4

was found to decrease by a factor of 3.6 and the peak instantaneous rate to decrease by a factor of 13. Larger reduction is obtained in our case because Pb is more effective than Li in slowing down high energy neutrons and C is more effective than Li in slowing down low energy neutrons. This implies that the wall protection concept used in the University of Wisconsin HIB fusion reactor design will be very effective in reducing damage to the first wall.

VI. Helium Production Rate

The instantaneous helium production rate in the protected ferritic steel first wall is given in Fig. 9. A peak instantaneous helium production rate of .173 appm/s occurs about 15 ns after the leading edge of the pulse arrives at the wall. The cumulative helium production is given in Fig. 10. It is clear that the time spread here is much smaller than that for the dpa. The reason is that the (n,α) reaction in iron has a threshold energy of $\sim$ 2.7 MeV and neutrons at energies greater than this energy exist in the first wall over a relatively short period. The instantaneous helium production rate in an unprotected wall is given in Fig. 11. Again the time spread in this case is determined primarily by the time of flight spread of source neutrons.

The effect of the porous tube first wall protection on the helium production is given in Table 3. The total helium production in a full power year is found to decrease by a factor of 370 while the peak instantaneous helium production rate is found to decrease by a larger factor of 1030. Since the helium production reaction is a high energy reaction, neutron slowing down in the blanket is found to have a pronounced effect on the total helium production in the wall.

VII. Energy Deposition Rate

The time dependent neutron and gamma fluxes are used together with the appropriate kerma factors for neutron and gamma energy deposition to calculate the energy deposition rate in the blanket and first wall. The results are given in Fig. 12 at the blanket first surface, the center of the blanket, and the first wall. The time distribution is very narrow at the first surface and broadens as one moves towards the first wall. While the time spread at the first surface is determined by the time of flight spread, the spread at the

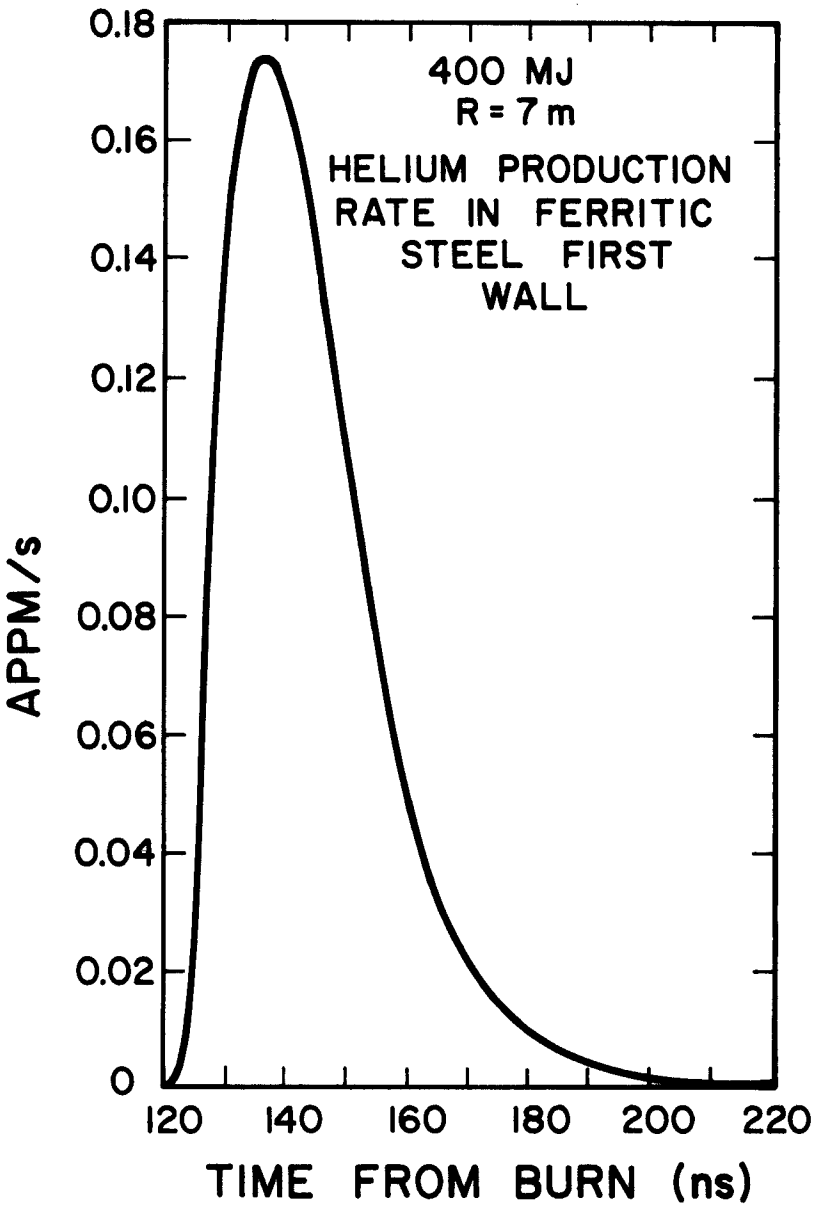

Fig. 9 Helium production rate in the protected first wall.

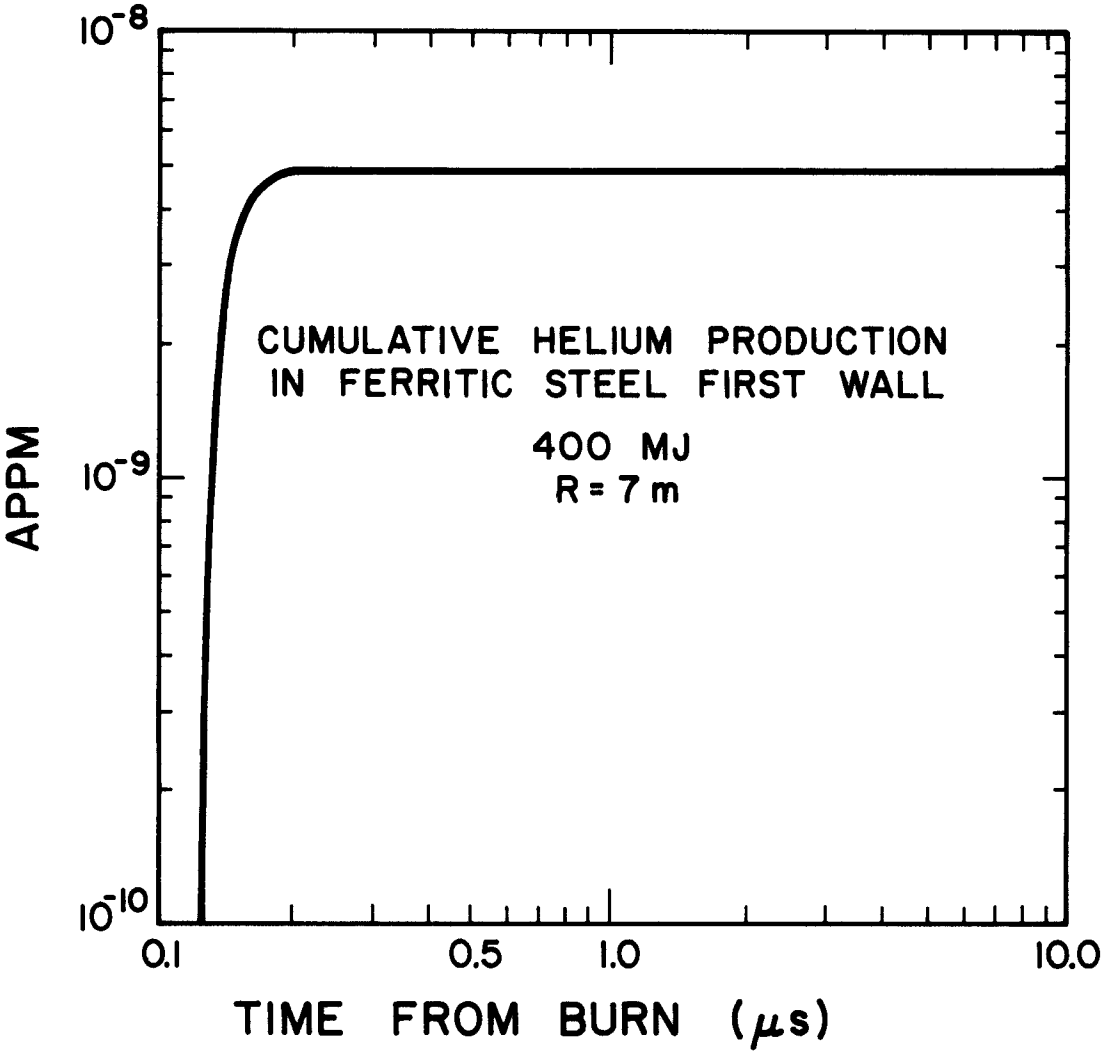

Fig. 10 Cumulative helium production in the protected first wall.

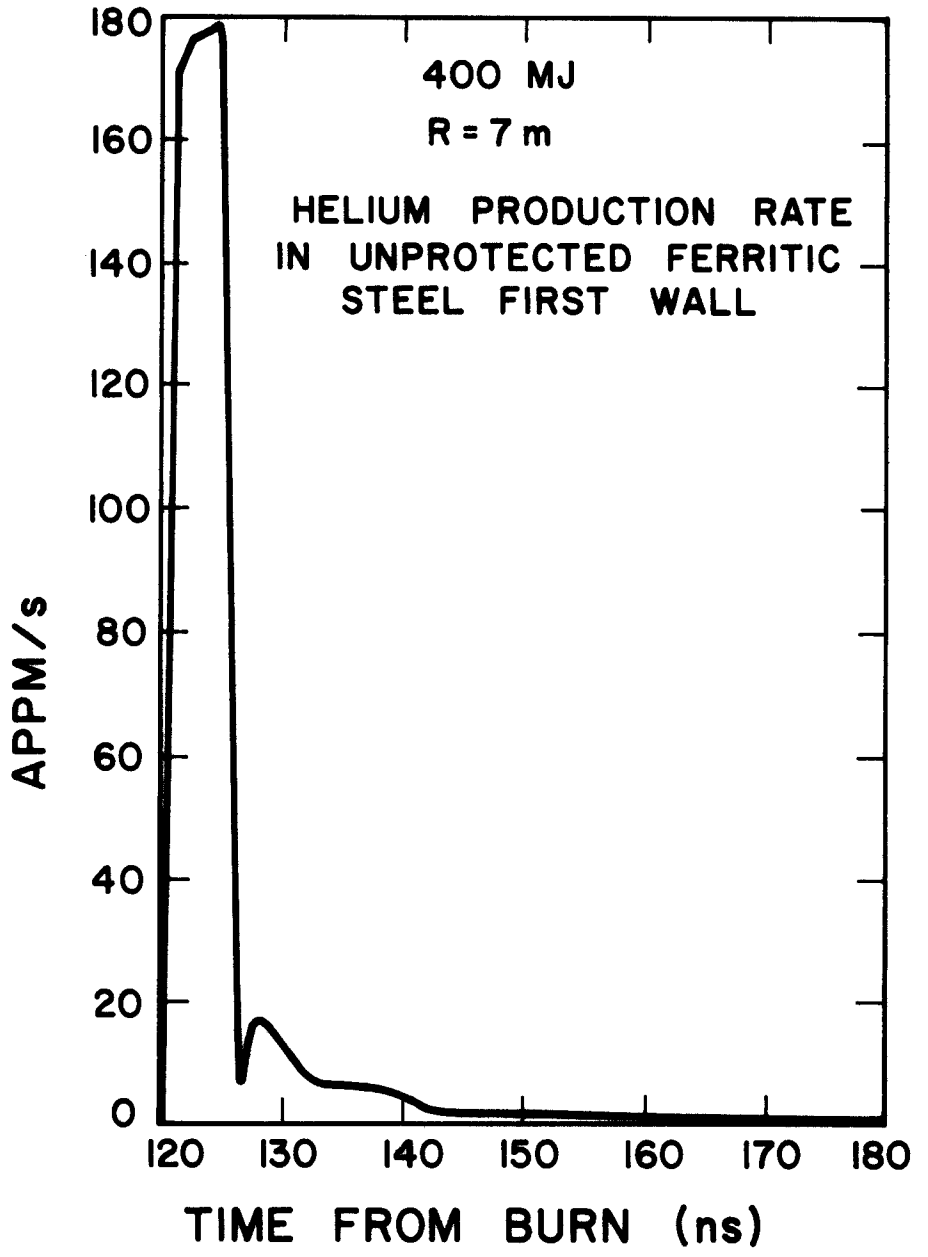

Fig. 11 Helium production rate in the unprotected first wall.

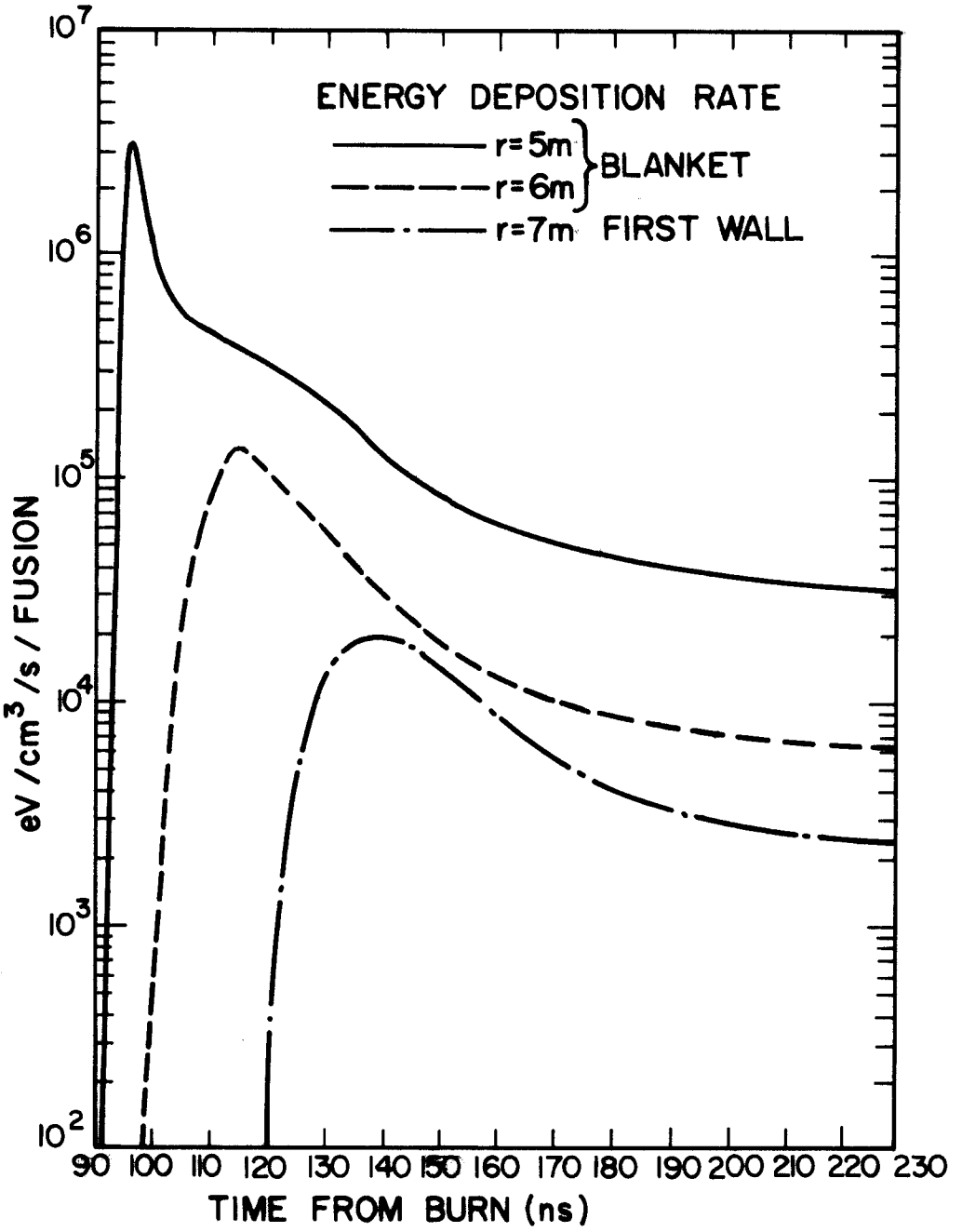

Fig. 12 Energy deposition rate in the HIB blanket and first wall.

Table 3

Effect of First Wall Protection on Helium Production

	Peak Instantaneous Helium Production Rate (appm/s)	Time Spread fwhm (ns)	Total Helium Production (appm/FPY)
Protected Wall	.173	26	2.07
Unprotected Wall	179	5	737

first wall is determined by the slowing down time in the blanket. For a 400 MJ fusion yield the peak instantaneous power densities in the blanket and the first wall are found to be 2.35×10^8 and 4.32×10^5 W/cm^3, respectively. This corresponds to peak to average temporal power density ratios of 9.2×10^6 and 1.4×10^5, respectively. The results in Fig. 13 give the instantaneous energy deposition rate in the unprotected first wall. The distribution is very narrow with a peak power density of 3.3×10^8 W/cm^3 for a 400 MJ fusion yield. The peak to average temporal power density ratio in the wall is found to be 1.1×10^7. The porous tube first wall protection concept is found to decrease the peak instantaneous power density in the wall by a factor of $\sim$ 760 and the total nuclear heating in the wall by a factor of $\sim$ 10. These results are useful for stress analysis studies.

VIII. Summary and Concluding Remarks

Time dependent neutronics analysis for the ferritic steel first wall of the University of Wisconsin heavy ion beam fusion reactor design has been performed. The analysis accounts for neutron interactions in the target

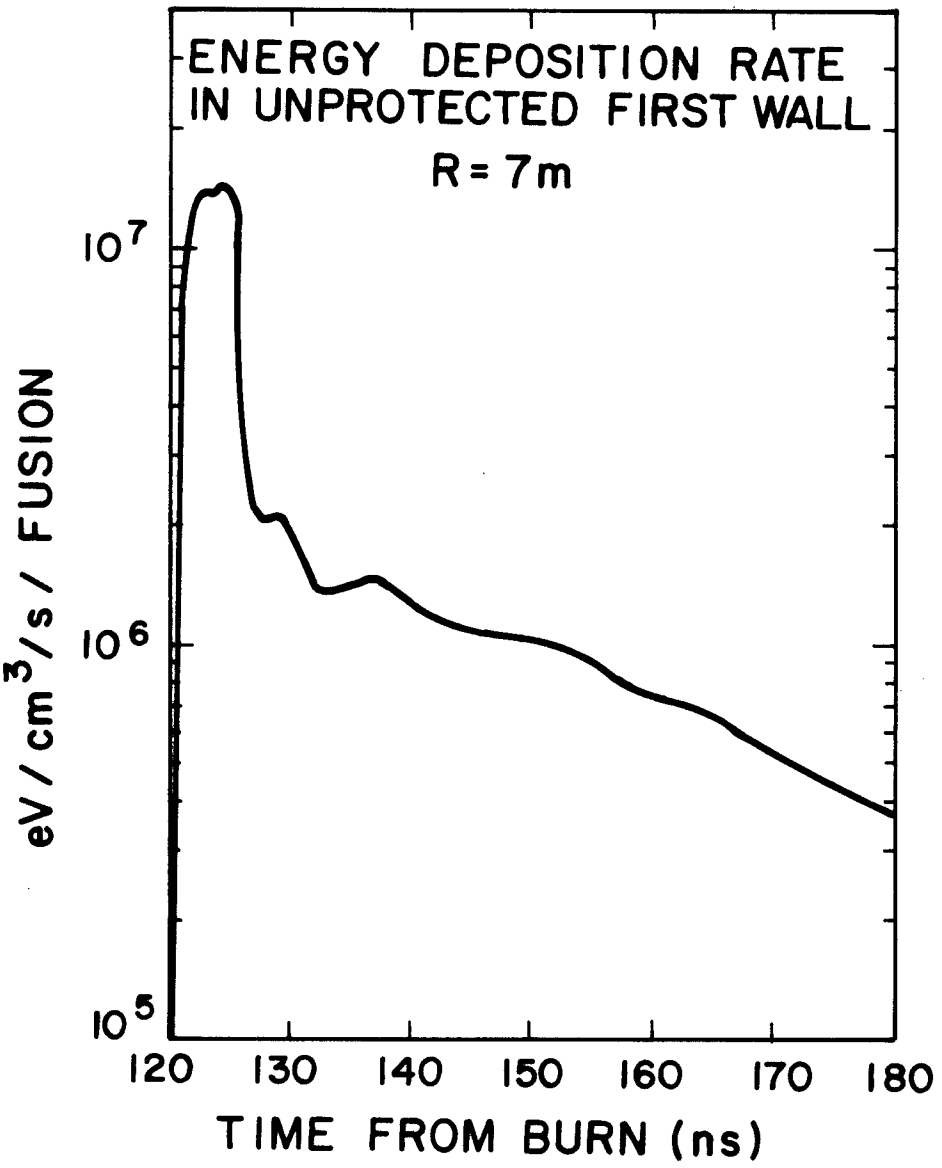

Fig. 13 Energy deposition rate in the unprotected first wall.

resulting in neutron multiplication and significant spectrum softening. The time dependence of the neutron source is modified in such a way that the multigroup treatment adopted in the time dependent transport code predicts the correct time of flight spread of neutrons in each group as they travel from the source to the first surface of the blanket. A modified version of the time dependent discrete ordinates code TDA has been used.

Neutron slowing down in the porous tube first wall protection system is found to have a significant effect on the time dependent spectrum and damage in the first wall. The time over which the damage occurs is found to be determined primarily by the slowing down time in the blanket. In the case of an unprotected wall, where no slowing down occurs in front of the wall, the spread is determined primarily by the time of flight spread.

Using the porous tube first wall protection concept results in significant reductions in peak instantaneous and total dpa and helium production rates. Our results show also that the peak power density in the first wall resulting from nuclear heating decreases considerably when the porous tube concept is used to protect the wall.

Acknowledgment

Funding for this work was provided by the Kernforschungszentrum Karlsruhe, Federal Republic of Germany.

References

1. N. Packen et al., J. Nucl. Mater., 78, 143 (1978).

2. N.M. Ghoniem and G.L. Kulcinski, Nucl. Engr. Design, 52, 111 (1979).

3. F. Beranek and R.W. Conn, UWFDM-310, University of Wisconsin (1979).

4. M.M. Ragheb and G.L. Kulcinski, Trans. Am. Nucl. Soc., 34, 644 (1980).

5. RSIC Code Package CCC-180, "TDA," Radiation Shielding Information Center, ORNL.

6. RSIC Code Package CCC-254, "ANISN-ORNL," Radiation Shielding Information Center, ORNL.

7. G.E. Bosler and T.G. Frank, Trans. Am. Nucl. Soc., 21, 16 (1975).

8. R. Bangerter and D. Meeker, LLL Report UCRL-50021-76, p. 4-44 (1980).

9. RSIC Data Library Collection, "VITAMIN-C, 171 Neutron, 36 Gamma-Ray Group Cross Section Library in AMPX Interface Format for Fusion Neutronics Studies," DLC-41, ORNL.

10. RSIC Data Library Collection, "MACKLIB-IV, 171 Neutron, 36 Gamma-Ray Group Kerma Factor Library," DLC-60, ORNL.